Earthquake Geotechnical Engineering for Protection and Development of Environment and Constructions – Silvestri & Moraci (Eds)
© 2019 Associazione Geotecnica Italiana, Rome, Italy, ISBN 978-0-367-14328-2

Cyclic response of artificially cemented soils

J.A. Mendoza, D. Lombardi, S.M Ahmad & B. Ismael
The University of Manchester, UK

ABSTRACT: This research work studies the cyclic response of artificially cemented sand samples. The material consists of fine silica sand, commercially known as Redhill 110; the cementation is induced by mixing the material with fast setting Portland cement and then applying the confining pressure. The bond formation is inferred from measurements of shear wave velocity using bender elements. It is observed that the shear wave velocity increases significantly in the first 20 hours from 130 MPa to 280 MPa. The sample is subsequently subjected to cyclic loading applied at a constant cyclic stress ratio (0.2). The results show an asymmetrical stress-strain curve that gradually moves towards large compressive strain. It is also noted that higher stiffness of the sample attributed to grain bonds is lost after the application of the first cycle of loading. The macroscopic behaviour observed in the cyclic triaxial test is finally discussed based on the microscopic features of the sample obtained from in X-Ray Computed Tomography Scanning with obtained images with voxel size of 4.998 μm.

1 INTRODUCTION

1.1 *Artificially cemented sands*

The amount of cement, confining stress, density, gradation and structure are governing variables in the behaviour of cemented soils according to Clough *et al.*, (1981). Saxena *et al.*, (1988) found that even a small amount of cement increases significantly the cyclic strength of uncemented sands and that the stress-strain curves are often asymmetrical about the zero strain axis. Similar findings were reported by Clough *et al.*, (1989) were the strength of cemented sands was found higher for both static and cyclic loads. One aspect, often disregarded, is the effect of changes in confining pressure in the small-strain stiffness of artificially cemented sands and the implications in the cyclic response. Fernandez and Santamarina, (2001) showed the degradation generated on the small-strain stiffness of artificially cemented samples cured under confining pressure, when subjected to changes of the initial curing stress. Consoli *et al.*, (2009) found that there is a relation between the peak strengths of an artificially cemented soil and the relationship void volume and cement volume.

In this study cemented samples were prepared by mixing Redhill-110 sand with fast setting Portland cement; these represented typical soil conditions of a cemented sand. The paper investigates the cyclic behaviour of these artificially cemented soils using a cyclic triaxial apparatus and bender element for accurate measurement of shear stiffness. Results show that cemented samples tends to become stiffer as cyclic loads progress. Artificially cemented soil samples have been used as an alternative to study the effect of cementation

in the mechanical response of soil, given that during sampling process of undisturbed samples, natural cemented soils can be subjected to partial and even complete decementation, which makes complicated to assess the effect of natural cementation in the low and large strain behaviour of the soil. Cementation of soils is a process that begins with the soil deposition and continues over time. These changes in fabric generate a different response to mechanical loads when compared to uncemented specimens.

2 MATERIALS AND EXPERIMENTAL METHODS

2.1 *Materials*

A mixture of sand and fast setting Portland cement was selected to create artificially cemented sand. The sand sample corresponds to Redhill-110 sand with the following index properties: $G_s = 2.65$, $e_{max} = 1.035$, $e_{min} = 0.608$, $D_{50} = 0.14$mm and angular shape. The cementing agent was fast setting Portland cement with a $G_s = 3.15$

2.2 *Sample preparation*

The specimen (50 mm diameter x 100 mm height) was prepared by initially mixing the relevant quantities of sand and cement in dry condition and then mixing them manually with water for 10 minutes. Next, the cement-sand mixture was statically compacted into 3 layers into the 50 mm split mound in the triaxial cell to a target void of 0.66 and moisture content of 19% with cement content of 5%. A sample with no cement addition and same void ratio was tested as well under the same conditions. The water content was fixed considering the cement content, so saturation was not achieved at any staged of the test. Mixing and compacting was achieved within 30 minutes of initial curing time, which is less that the setting time of the fast setting Portland cement (3 hours). Once compacted into the mould, the samples were let to cure for 72 hours under a constant confining pressure of 200 kPa. Samples of 75 mm diameter and 150 mm height were prepared using the same procedure to monitor the changes in small-strain stiffness G_o as cementation took place and then monitor G degradation under monotonic shearing.

2.3 *Experimental method*

The samples were tested under an undrained – unconsolidated (UU) test condition in a Bishop Type triaxial cell manufactured by GDS Instruments and equipped with an internal load cell. A one-way cyclic loading test with a stress ratio (S) of 0.2 and a period of 30 minutes was applied to the cemented and uncemented sample subjected to the curing confining pressure of 200 kPa. The test was conducted under a stress controlled configuration. A monotonic test was also performed on a 75mm diameter and 150mm height sample with a computer strain controlled triaxial cell manufactured by GDS where bender element allowed monitoring the degradation of stiffness during shearing. Undrained monotonic shearing was performed at a strain rate of 0.013%/min. Shear wave velocities were measured using a source wave with a frequency of 12.5 kHz. Arrival time was selected using cross-correlation. The UU test condition was selected to avoid damage to the cement matrix in the sample given that changes in confining pressure during consolidation and saturation stages can degrade the small-strain stiffness of the cemented samples. The microstructure of a cemented sample was studied using a Nikon Metrology 225/320 kV computed tomography in the Manchester Henry Moseley X-Ray Imaging Facility of The University of Manchester. The sample scanned had a diameter of 12.24mm and height of 20.32mm. The image resolution was 3192 x 3192 pixels and the voxel size of the images obtained was 4.998 μm. A cubic subvolume of 15.625 mm^3 (2.5 mm x 2.5 mm x 2.5 mm) was obtained from the centre of the sample to analyse and segment the phases present in the sample.

3 RESULTS

3.1 *Evolution of small strain stiffness*

The evolution of the small strain stiffness G_o is presented in Figure 1. The shear wave velocity was measured using bender element. The time difference between the transmission and reception represents the travel time through the sample from which the shear wave velocity can be calculated and hence the elastic shear modulus of the soils as described by Equation 1 below:

$$G_o = \rho V_s^2 = \rho\left(\frac{L^2}{t^2}\right) \tag{1}$$

where ρ= total mass density of the soil; L=tip to tip length between bender elements; V_s=shear wave velocity; and t= travel time of the shear wave. Shear waves were propagated vertically and cross-correlation was used to interpret and estimate the arrival time of the response wave. A G_o of 139 MPa corresponds to an uncemented sand under a confining pressure of 200 kPa, whereas G_o of 285 MPa was achieved by a cemented sand with 5% cement content cured under a confining pressure of 200 kPa. There a significant increase in G_o during the first 10 hours of curing time and after 20 hours of curing time there is no significant increase in stiffness. Shear wave velocity was measured every hour for 72 hours prior to shearing of the sample under undrained conditions.

Figure 2 shows the degradation of stiffness under monotonic load in a strain controlled test. Elastic shear modulus of the cemented sample (G) at a given axial strain (ε) was calculated and compared to the elastic shear modulus at small strain (G_o). After axial strain of 1%, the ratio G/G_o decreases at a higher rate compared to the degradation at 0.1% axial strain. The elastic shear modulus of the soil (G) was measure until a 15% axial strain where the ratio G/G_o reaches a value of less than 0.5. This behaviour could be indication of changes in the internal structure of the cemented sand and. Given that the cemented sample is composed by two different solid particles (silica grains and cement bonds) it exhibited a more brittle failure compared to the sample with no cement content under monotonic load, the higher rate of change of the ratio G/G_o could be attributed to the cement bonds having a brittle failure near the 1% strain.

3.2 *Cyclic triaxial test*

The undrained stress-strain responses of a sand sample with 5% cement content and a sample without cement addition under a stress controlled one-way cyclic loading test are shown in

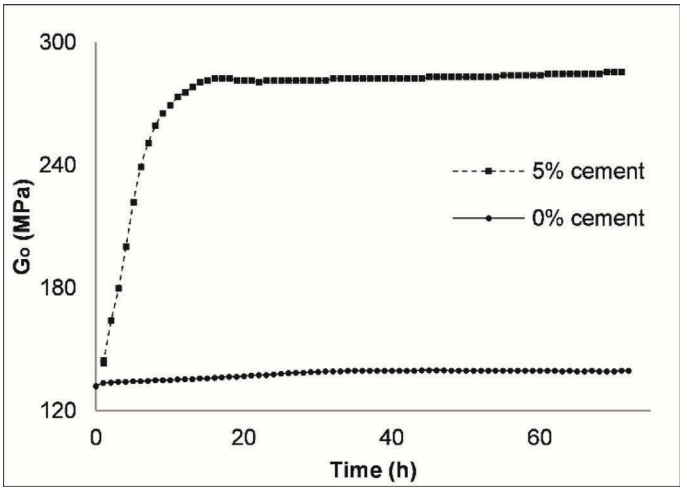

Figure 1. Evolution of stiffness during curing.

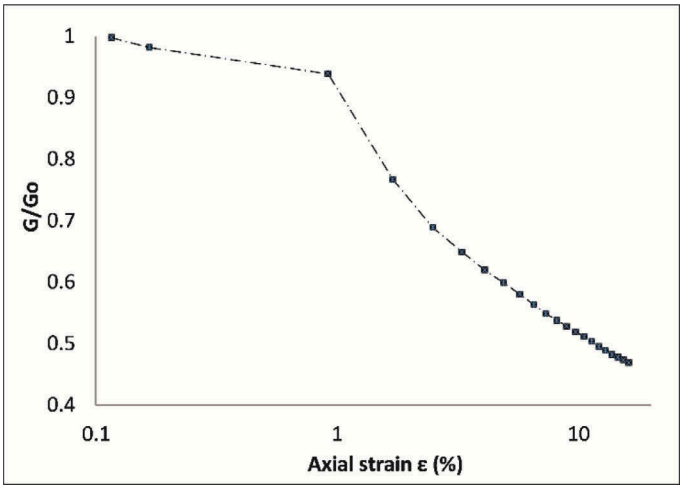

Figure 2. Degradation of stiffness under monotonic load in a 5% cement content sample.

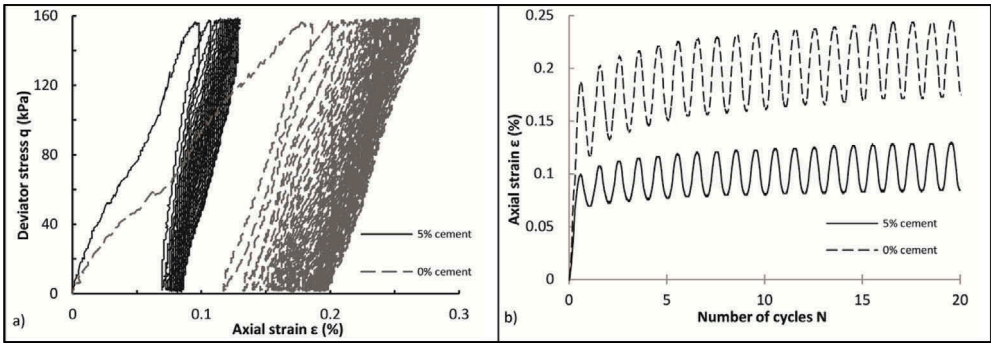

Figure 3. a) Stress-strain response of artificially cemented sand and uncemented sand. b) Strain accumulation after 20 cycles for a cemented and uncemented sample.

Figure 3a. After 20 cycles the increase in accumulated deformation was not significant for the cemented sample, being the maximum axial strain less than half than the uncemented sample (0.12% for a cemented sample and 0.26% for an uncemented sample) which indicated that the addition of cement reduces the accumulated strain. It is clear that the first cycle shows a different response than the consequent cycles. Most of the strain occurred during the first load-unload cycle and the graph shows an asymmetry increase in strain in both samples. The cemented sample shows a stiffer response in the first and subsequent cycles compared to the sample without cement addition. Figure 3b shows the strain variation due to the cyclic load against number of cycles where a greater increase in strain is reached within the first cycles. This effect can be seen in Figure 4, where the accumulated cyclic strain ($\Delta\varepsilon/\varepsilon$) versus normalised number of cycles (N/Nmax) is plot to visualize the strain accumulation on each cycle.

The slope of the stress-strain curve is observed to increase after the first cycle. Cycle 1 shows a slope similar to the monotonic test performed for a similar sample.

3.3 *X-Ray computed tomography*

The scanning arrangement inside the Nikon Metrology 225/320 kV computed tomography and a 3D reconstruction of the subvolume are shown in Figure 5. Three main phases can be

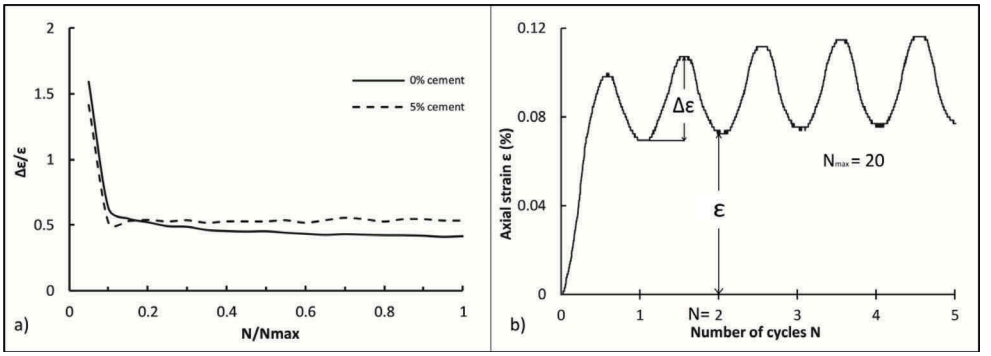

Figure 4. a) Accumulated cyclic strain versus normalised number of cycles. b) Schematic showing the parameters $\Delta\varepsilon$, ε, N and N_{max}.

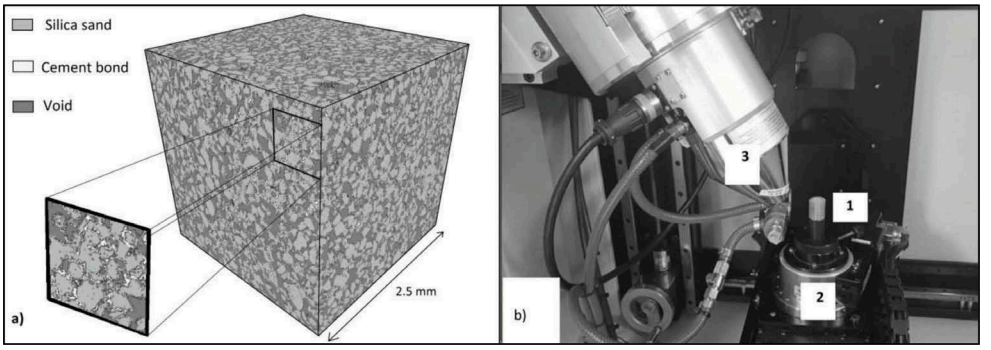

Figure 5. a) 3D volume reconstruction of cemented sample. Each side corresponds to a section of 2.5 mm x 2.5 mm. b) Inside of the Nikon Metrology 225/320 kV showing the cemented sample (1), the rotary stage (2) and the X-Ray source (3).

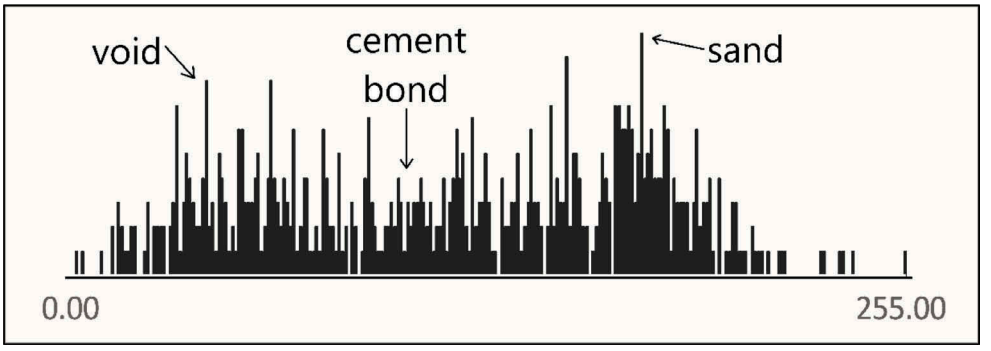

Figure 6. Histogram of the cemented sample indicating the intensities used to separate the phases found during the X-Ray CT scanning.

identified as Redhill-110 sand, cement bonds and voids. Light grey represents the grains of Redhill-110, dark grey represents the voids within the sample and the white areas clustered between contact points of sand grains represent the cement bonds. Figure 6 shows the grey-level histogram used to separate the three phases. Table 1 shows the computed volume

Table 1. Computed volumes of the phases within the cemented sample.

Material	Volume (mm^3)	Mean intensity
Sand	8.532145702	174
Cement bond	3.134324369	102
Void	4.016445503	43

V_p= 11.666470071 mm^3 V_v=4.016445503 mm^3 e= 0.344272558

corresponding to each of the phases. The total volume of the three phases is 15.682mm^3. The void ratio (e) of the analysed sample is calculated as described in Equation 2, where the volume of the solids (V_p) is divided by the volume of the void (V_v).

$$e = \frac{V_p}{V_v} \tag{2}$$

The void ratio for the cemented sample resulted in e = 0.34 which is lower that the target void ratio of the prepared samples (e=0.66). The formation of the cement bonds seems to decrease the initial voids of the sample as well as to increase the contact points between the sand grains, which would contribute to the increase in small-strain stiffness and the smaller accumulated strains during cyclic loading.

4 DISCUSSION

The response of artificially cemented sand with 5% of fast setting Portland cement was presented in Figure 3. It is worth nothing the asymmetry of the stress-strain curve, which indicates a stiffening of the soils as cyclic load continues.

The behaviour of the sample after 10 cycles seems to stabilize and moreover, the slope of the stress-strain curve of every cycle increased from cycle 1 to cycle 20 for both cemented and uncemented sample. As strain increases, the stiffness of the soil is expected to degrade, as shown in Figure 1 where the degradation of $\mathbf{G_o}$ was monitored for strains up to 15%, however, the artificially cemented sand seems to become stiffer after the first cycle loading. The accumulation of strain in the direction of the load applied, known as ratcheting as described in Ghionna and Porcino, (2006), can also be observed.

The effects of bond breakage can be considered to explain this behaviour in artificially cemented soils. Given the brittle behaviour of cemented sands, once the bonds are broken, the strength is provided by the sand grains, which would lead to a rearrange of particles under cyclic load.

The effects of cementation degradation in stiffness of artificially cemented sands have been studied by Baig et al., (1997) and Fernandez and Santamarina, (2001) showing that changes in isotropic confinement can cause decementation (bond breakage).

The void ratio computed during the X-Ray CT scanning showed to be lower than the target void ratio of the sample and even lower than the $e_{min} = 0.608$ for this sand. This can be attributed to the creation of the cement bonds during the curing and would explain the increase in small-strain stiffness and the smaller strain accumulation for the cemented sample. The histogram showed than separating the solid phase from the voids is easier than separate sand from cement bonds. A more detailed analysis can be used to obtained a more accurate separation of the sand and cement phases. However, the volume of solids would remain constant even with a more detailed analysis and hence the void ratio is expected to be very similar to $e = 0.34$ since solids and voids are well differentiated in the grey intensity histogram.

5 CONCLUSIONS

Undrained cyclic stress-strain behaviour of artificially cemented sand with 5% of cement content leads to the following conclusions:

1. Larger strains are expected in the first cyclic loading of the artificially cemented sample and smaller strains for consecutive cycles.
2. Increase in cement content decreases the strain accumulation (Ratcheting) under the same loading condition for a given relative density when compared to an uncemented sample.
3. Artificially cemented sand tends to become stiffer after the first cyclic load.
4. Stiffening of the samples can be attributed to the changes in structure cause by the degradation of the cementing bonds.
5. From the microstructural analysis, it can be seen that cement bonds are mainly formed in contact points between the silica grains. The computed volume of solids and volume of voids showed decrease of the void ratio from the initial condition in the cemented sample. Additional imaging analysis, such as the Scanning Electron Microscope can be used to confirm and further analyse the presence of the cement bonds and the effect of the void ratio of the samples.
6. Particular care has to be put during the docking of cemented samples to apply two-way cyclic loading, since changes in isotropic confinement have been reported to cause cementation degradation. One-way cyclic loading is advised as preferred cyclic loading test, as it would minimise damaging of the sample by accidental changes in confining pressure.

REFERENCES

Baig, S., Picornell, M. and Nazarian, S. (1997) 'Low Strain Shear Moduli of Cemented Sands', *Journal of Geotechnical and Geoenvironmental Engineering*, 123(6), pp. 540–545. doi: 10.1061/(ASCE)1090-0241(1997)123:6(540).

Clough, G. W. *et al*. (1989) 'Influence of Cementation on Liquefaction of Sands', *Journal of Geotechnical Engineering*, 115(8), pp. 1102–1117. doi: 10.1061/(ASCE)0733-9410(1989)115:8(1102).

Clough, G. W., Sitar, N. and Bachus, R. C. (1981) 'Cemented Sands under Static Loading', *Journal of the Geotechnical Engineering Division*. ASCE, 107(GT6), pp. 799–817. Available at: https://ci.nii.ac.jp/naid/10012757289/ (Accessed: 22 September 2018).

Consoli, N. C. *et al*. (2009) 'Fundamental Parameters for the Stiffness and Strength Control of Artificially Cemented Sand', *Journal of Geotechnical and Geoenvironmental Engineering*, 135(9), pp. 1347–1353. doi: 10.1061/(ASCE)GT.1943-5606.0000008.

Fernandez, A. L. and Santamarina, J. C. (2001) 'Effect of cementation on the small-strain parameters of sands', *Canadian Geotechnical Journal*. NRC Research Press Ottawa, Canada, 38(1), pp. 191–199. doi: 10.1139/cgj-38-1-191.

Ghionna, V. N. and Porcino, D. (2006) 'Liquefaction Resistance of Undisturbed and Reconstituted Samples of a Natural Coarse Sand from Undrained Cyclic Triaxial Tests', *Journal of Geotechnical and Geoenvironmental Engineering*, 132(2), pp. 194–202. doi: 10.1061/(ASCE)1090-0241(2006)132:2(194).

Saxena, S. K., Reddy, K. R. and Avramidis, A. S. (1988) 'Liquefaction Resistance of Artificially Cemented Sand', *Journal of Geotechnical Engineering*, 114(12), pp. 1395–1413. doi: 10.1061/(ASCE)0733-9410(1988)114:12(1395).